

9195

NACA TN 2861

NATIONAL ADVISORY COMMITTEE FOR AERONAUTICS

TECHNICAL NOTE 2861

ANALYTICAL INVESTIGATION OF ICING LIMIT FOR DIAMOND-SHAPED
AIRFOIL IN TRANSONIC AND SUPERSONIC FLOW

By Edmund E. Callaghan and John S. Serafini

Lewis Flight Propulsion Laboratory
Cleveland, Ohio



Washington
January 1953

AFMDC
AERONAUTICAL LIBRARY
AFL 2811

2861



0065808

1J

NATIONAL ADVISORY COMMITTEE FOR AERONAUTICS

TECHNICAL NOTE 2861

ANALYTICAL INVESTIGATION OF ICING LIMIT FOR DIAMOND-SHAPED
AIRFOIL IN TRANSONIC AND SUPERSONIC FLOW2
40/2

By Edmund E. Callaghan and John S. Serafini

SUMMARY

Calculations have been made for the icing limit of a diamond airfoil at zero angle of attack in terms of the stream Mach number, stream temperature, and pressure altitude. The icing limit is defined as a wetted-surface temperature of 32° F and is related to the stream conditions by the method of Hardy.

The results show that the point most likely to ice on the airfoil lies immediately behind the shoulder and is subject to possible icing at Mach numbers as high as 1.4.

INTRODUCTION

As the operational speed of aircraft is increased through the transonic region, the frictional heating available to prevent the formation of ice on the aircraft becomes an important quantity. A study of the probable icing limits of a high-speed airfoil in transonic and supersonic flow was made in terms of the pertinent variables of flight Mach number and free-stream conditions of pressure and temperature. The procedure used to determine the icing limit is based on the method presented in reference 1 for calculating the surface temperature of an insulated body (a body within which heat is not conducted from one section to another) running fully wet in an air stream. The icing limit at any point on the airfoil was assumed to depend upon maintaining a temperature of 32° F at that point. The free-stream static temperature corresponding to this icing limit was calculated for each point on the airfoil for particular values of free-stream Mach number and pressure.

The results presented herein were calculated for a symmetrical diamond airfoil at zero angle of attack for a range of airfoil-thickness ratios from 0.02 to 0.10, pressure altitude from sea level to 45,000 feet, and free-stream static temperatures to -40° F.

SYMBOLS

The following symbols are used in this report:

c_p specific heat of air at constant pressure, Btu/(lb)(°F)
 e vapor pressure, lb/sq ft
 k_e coefficient of evaporation
 k_h coefficient of heat transfer
 L latent heat of vaporization, Btu/lb
 M Mach number
 m_a molecular weight of air
 m_e molecular weight of water vapor
 p static pressure, lb/sq ft
 r recovery factor
 T static temperature, °R
 t/c airfoil thickness ratio, ratio of airfoil maximum thickness to chord
 $T_{0,c}$ minimum free-stream static temperature corresponding to ice-free condition on surface as defined in equation (1a), °R
 ΔT_1 temperature increment resulting from frictional heating in the boundary layer, °R
 γ ratio of specific heats of air, 1.400

Subscripts:

0 free-stream static conditions
1 local conditions at the edge of boundary layer
s surface

ANALYSIS

2704

The method of reference 1 offers a convenient means for determining the local surface temperature on a wetted body as a function of the free-stream conditions of temperature, pressure, vapor pressure, and velocity, provided the flow field about the body is known. Ease of calculation was achieved by a number of simplifying assumptions. The restrictions caused by these assumptions will be discussed in relation to the general heat balance for an unheated body flying through icing conditions.

Several investigators have made quite complete analyses of the heat balance for a body flying through a cloud (references 2 and 3). The generalized heat balance for such conditions is well known and has been stated quite concisely by Messinger (reference 2). Some simplification of the general equation may be obtained by considering the case of an insulated body subjected to sufficient frictional heating to maintain the surface ice free. In this case, the heat balance is as follows:

(1) Heat due to the frictional, or viscous, effects

plus

(2) Heat due to the kinetic energy of the water droplets

plus

(3) Heat of fusion

equals

(4) Heat lost by convection

plus

(5) Heat for evaporation of water

plus

(6) Heat required to raise temperature of water droplets from stream temperature to surface temperature

The result of Hardy's relation (reference 1) is obtained by equating the frictional term (1) to the sum of the convective term (4) and the evaporation term (5). For Hardy's relation to be valid, terms (2) and (3) must be small compared with term (1), and term (6) must be small compared with term (4) or (5); or the sum of terms (2) and (3) must be nearly equal to term (6).

The heat of fusion term (3) offers considerable complication to the problem. It is conceivable that the surface film might consist of a mixture of water and ice particles without ice actually adhering to the surface. The heat of fusion would necessarily have to be withdrawn from a portion of the film for such particles to occur and, because of the lack of knowledge of the percentage of the film that might be frozen before visible icing occurs, it would appear advisable to define an ice-free surface as being fully wet at 32° F with no ice particles in the film. This definition for the icing limit eliminates term (3) from the general heat balance and Hardy's relation becomes applicable if term (2) is approximately equal to term (6) or both are negligible. Term (2) is directly proportional to the impingement rate and the square of the flight speed; term (6) is directly proportional to the impingement rate and the temperature difference between the stream and the surface. If the impingement rate is small, as for the case of low liquid-water contents, then both terms (2) and (6) are negligible. For calculations of the icing limit, both terms are of the same order of magnitude and because of the nature of the problem the temperature difference between the surface and the stream increases with increasing flight speed. Both terms therefore increase with increasing Mach number; large values for either term are only encountered at large values of liquid-water content and flight speed. Such a combination is highly improbable in actual flight since high speeds usually occur at high altitudes, and high altitudes imply small liquid-water contents.

The relation of Hardy applies in particular to a surface barely wetted with a very thin film free of ice particles but is probably nearly correct for the whole range of practical interest for high-speed flight.

Method of Calculation

Wetted-surface temperature. - The equation for the temperature of a wetted surface in an air stream developed in reference 1 was written as

$$T_1 - T_s + \Delta T_1 = \frac{k_e m_e}{k_h m_a} \left(\frac{e_s}{p_1 - e_s} - \frac{e_1}{p_1 - e_1} \right) \frac{L}{c_p} \quad (1)$$

where the subscript s refers to conditions at the surface and subscript 1 to conditions at the edge of the boundary layer. From the energy relation for a viscous fluid

$$T_1 + \Delta T_1 = T_1 \left[1 + \frac{r(r-1)}{2} M_1^2 \right]$$

Substituting this relation in equation (1) and solving for T_s yields

$$T_s = T_1 \left[1 + \frac{r(\gamma - 1)}{2} M_1^2 \right] - \frac{k_e m_e L}{k_h m_a c_p} \left(\frac{e_s}{p_1 - e_s} - \frac{e_1}{p_1 - e_1} \right)$$

Because interest in this problem is fixed on a definition of flight circumstances that provide local surface temperatures of 32° F, the terms T_s , L , and e_s are constants. Hardy observed (reference 1) that for the range of temperatures near 32° F the ratio of the evaporation coefficient k_e to the heat-transfer coefficient k_h was very nearly 1. A solution of equation (1) can be obtained for any one of the four variables (e_1 , p_1 , M_1 , and T_1) provided the other three are known.

From purely physical reasoning, however, an additional restriction exists. This restriction results from the fact that the air in a cloud is fully saturated at the static or free-stream conditions. For each value of stream-static temperature, the free-stream vapor pressure is therefore assumed a constant and equal to the saturated vapor pressure. If it is assumed that the flow about the body, outside the boundary layer, is accomplished with no change in phase, that is, no condensation or evaporation, then Dalton's law of partial pressures applies and

$$\frac{e_1}{e_0} = \frac{p_1}{p_0}$$

If a reasonable value of the recovery factor r is assumed, say 0.88, then equation (1) may be rewritten in the form shown below

$$492 = \frac{T_1 (1 + 0.176 M_1^2)}{T_{0,c}} - 2776.5 \left[\frac{12.75}{\left(\frac{p_1}{p_0} - 12.75 \right)} - \frac{e_0}{(p_0 - e_0)} \right] \quad (1a)$$

which is quite convenient for purposes of calculation because $T_1/T_{0,c} (1 + 0.176 M_1^2)$ and p_1/p_0 can be readily calculated for each point on a diamond airfoil.

Because e_0 is a function of $T_{0,c}$, the solution of equation (1a) must be solved by trial and error. In an effort to reduce the laboriousness of such calculations, a number of charts similar to that shown in figure 1 were made. For each pressure altitude considered, the free-stream static temperature corresponding to an ice-free condition $T_{0,c}$ was plotted as a function of the parameter $T_1/T_{0,c} (1 + 0.176 M_1^2)$ by means of equation (1a) for constant values of the pressure ratio p_1/p_0 . For each value of p_1/p_0 and $T_1/T_{0,c} (1 + 0.176 M_1^2)$ a free-stream static temperature which corresponds to a surface temperature of 32° F and therefore represents the minimum free-stream temperature for an ice-free surface $T_{0,c}$ is obtained. The lower limit of free-stream static

temperature was considered to be -40° F for the purposes of these calculations since it has been shown (references 4 and 5) that supercooled water droplets are not likely to be found at temperatures below this value.

Flow-field calculations. - The flow field about a diamond or double-wedge profile can be characterized in general by four regions; a subsonic region, a subsonic region with sonic velocity at the shoulder, a mixed subsonic-supersonic region with a detached bow wave, and a supersonic region with attached shock waves. The regions of most interest are in the currently important ranges of transonic and supersonic flight and the results presented herein will be limited thereto.

A recent analysis is given in references 6 and 7 for the subsonic region with a sonic line at the shoulder. This solution is for a thin, symmetrical wedge at zero angle of attack followed by a straight section. The results in this region presented herein are therefore limited to the front half of the diamond airfoil.

The mixed subsonic-supersonic region with detached bow wave has been solved in references 8 and 9. This solution applies to a thin, symmetrical diamond airfoil at zero angle of attack for Mach numbers from 1 to the Mach number at which the shock attaches. The flow in this region is subsonic over the front half of the airfoil increasing to sonic velocity at the shoulder. The flow then expands supersonically around the corner, and supersonic flow exists over the back half of the airfoil to the trailing edge.

The flow about a diamond airfoil in purely supersonic flow has been known for many years. The results used herein are those of reference 10 because of their ease in use and applicability. The flow in this region is supersonic over the front half of the airfoil with an expansion region at the shoulder and a consequent higher Mach number on the back surface of the airfoil, the velocities and pressures being constant over each surface for a particular value of airfoil thickness and stream Mach number.

The calculation of the chordwise pressure and Mach number distributions over a symmetrical-diamond airfoil of specific thickness ratio t/c at zero angle of attack through the entire transonic-supersonic range can therefore be accomplished by combining the results of references 6 to 10.

The analyses of references 7 to 9 were made using a speed function ξ and a generalized pressure coefficient \tilde{C}_p . The results of these analyses are presented graphically by plots of the chordwise distribution of ξ and \tilde{C}_p for constant values of the free-stream speed function ξ_0 . The pressure ratio p_1/p_0 is related to the generalized pressure coefficient \tilde{C}_p by the equation

$$\frac{p_1}{p_0} = 1 + \frac{\frac{\gamma M_0^2}{2} \left(\frac{t}{c}\right)^{\frac{2}{3}} \tilde{c}_p}{2(\gamma + 1)^{\frac{5}{3}}}$$

The Mach number, either local or free stream, is related to the speed function ξ by the equation

$$M = \sqrt{1 + \xi \left[(\gamma + 1) \left(\frac{t}{c} \right)^{\frac{2}{3}} \right]^{\frac{2}{3}}}$$

The temperature ratio T_1/T_0 is obtained from the energy relations for a compressible fluid and is given in terms of Mach number by the equation

$$\frac{T_1}{T_0} = \frac{1 + \frac{\gamma - 1}{2} M_0^2}{1 + \frac{\gamma - 1}{2} M_1^2}$$

An example of a typical calculation of $T_{0,c}$ at a particular chordwise position is given for the 25-percent chord station and a value of the free-stream speed function ξ_0 of 0.703. Values of ξ of -0.740 and C_p of 2.890 are obtained from figures 3 and 5, respectively, of reference 8. If t/c of 0.06 is assumed, then $M_0 = 1.092$, $M_1 = 0.8926$, $p_1/p_0 = 1.276$, $T_1/T_0 = 1.068$, and $T_1/T_0 (1 + 0.176 M_1^2) = 1.218$. At a pressure altitude of 15,000 feet, a $T_{0,c}$ of 422.5° R is obtained from figure 1.

For the supersonic case with an attached shock (reference 10), the values of p_1/p_0 and M_1/M_0 can be obtained directly from the charts of the reference report and, hence, the calculation of the parameters required for obtaining $T_{0,c}$ from figure 1 is simple.

RESULTS AND DISCUSSION

For each value of airfoil thickness ratio and free-stream Mach number assumed, the values of the parameters $T_1/T_0 (1 + 0.176 M_1^2)$ and p_1/p_0 can be calculated over the whole range of transonic and supersonic speeds. At each pressure altitude, the free-stream static temperature $T_{0,c}$ corresponding to a wetted surface temperature of 32° F (ice free) can then be obtained from charts similar to figure 1.

This value of $T_{0,c}$ corresponds to the lowest free-stream static temperature T_0 which will give ice-free conditions at the particular point on the airfoil under consideration for the given values of free-stream Mach number and pressure altitude.

A plot of $T_{0,c}$ as a function of the chordwise distance is shown in figure 2 for several free-stream Mach numbers for a 4-percent-thick symmetrical-diamond airfoil at zero angle of attack and a pressure altitude of 30,000 feet.

A study of figure 2 shows that the general trend of the curves is very similar for Mach numbers from 0.7593 to 1.105, that is, from the subsonic region to the supersonic region with attached shock. For each curve the minimum $T_{0,c}$ increases slowly from the leading edge to the midchord. The sudden jump in the free-stream static temperature required for icing protection at the midchord results from the expansion around the corner and the consequent decrease in local static pressure and increase in local velocity. The increase in velocity and the decrease in pressure enhance the evaporation, hence, the increase in the required $T_{0,c}$. Water impinging on the front half of the airfoil might therefore run back along the surface, spill around the shoulder, and freeze. Downstream of the shoulder, the free-stream temperature required for protection decreases slowly to the trailing edge.

When the shock wave is attached and the flow is everywhere supersonic ($M_0 = 1.2$, or greater), the free-stream temperature for protection is a constant for the whole front surface and the whole back surface. The free-stream temperature required for protection of the back half is, however, greater for the reasons previously cited.

This and similar figures for other altitudes and airfoil thickness ratios show that the critical points for these airfoils are immediately ahead of the shoulder for the front half of the airfoil and immediately behind the shoulder for the back half of the airfoil. The icing limit for these two critical points is shown in figure 3(a) where the minimum free-stream temperature corresponding to an ice-free condition is shown as a function of the free-stream Mach number for pressure altitudes of sea level and 30,000 feet for a 6-percent-thick airfoil. The value of $T_{0,c}$ decreases rapidly with increasing Mach number; that is, the temperature region of possible icing hazard becomes much smaller with increasing Mach number. The free-stream static temperatures required for protection apparently are higher at the higher pressure altitudes as would be expected since, with other conditions equal, the decreased pressure enhances the evaporation rate. At a pressure altitude of 30,000 feet the curve shown for the critical point behind the shoulder indicates the possibility of icing at a Mach number approaching 1.4.

The effect of altitude is shown clearly in figure 3(b) for free-stream Mach numbers of 0.67, 1.0, and 1.3 for the critical point ahead of the shoulder on the front surface and for Mach numbers of 1.0 and 1.3 for the point immediately behind the shoulder. At a particular value of Mach number the curves for both critical points remain nearly parallel over the altitude range. For Mach numbers of 1.0 or less the free-stream temperature required for protection increases with increasing altitude with a definite decrease in the slope of the curves in the higher altitude range. For the higher Mach numbers the slope of the curves increase over the whole range from sea level to 45,000 feet.

The effect of airfoil thickness on the icing limit for the two critical points on the airfoil is shown in figure 3(c) where the free-stream temperature required for protection is plotted as a function of the airfoil thickness ratio. The icing limit at a pressure altitude of 45,000 feet is shown for the point ahead of the shoulder for free-stream Mach numbers of 0.875, 1.00, and 1.30 and for the point immediately behind the shoulder for Mach numbers of 1.0 and 1.3. For the point ahead of the shoulder, the temperature required for protection remains constant or decreases with increasing thickness depending on the Mach number. For the point immediately behind the shoulder, the temperature required for protection increases with increasing thickness.

An increase in $T_{0,c}$ of approximately 20° R resulted when the thickness ratio increased from 0.02 to 0.10 for the critical point behind the shoulder at a free-stream Mach number of 1.00. A decrease in $T_{0,c}$ of approximately 14.5° R resulted when the thickness ratio increased from 0.02 to 0.10 for the critical point ahead of the shoulder at a free-stream Mach number of 1.30.

Experimental verification of the results presented herein has been obtained from data taken in a 4- by 10-inch duct tunnel at a free-stream Mach number of 1.36 with a 6.82-percent-thick symmetrical-diamond airfoil of 5.50-inch chord at zero angle of attack. The icing limit was determined by successively raising the free-stream static temperature until no ice formed on the surface. The results of these tests are summarized in the following table and compared with results calculated by the analytical method presented herein:

P_0 (in. Hg)	Minimum free-stream static temperature corresponding to ice-free condition, $T_{0,c}$			
	Experimental		Analytical	
	Front surface	Back surface	Front surface	Back surface
9.13	404	---	403	---
9.41	---	422	---	422
9.76	406	---	401	---
9.91	---	418	---	422
3.91	---	---	447	---

The excellent agreement obtained in several cases is probably somewhat fortuitous since the experimental error was estimated to be $\pm 10^{\circ}$ F. These results, however, show that the calculated icing limit is very closely approximated experimentally and, hence, provides considerable credence for the calculations presented herein. The run-back icing on the rear surface, which was indicated by the analysis, was also observed experimentally. Visual observations of the model showed that the surface water film flowed smoothly around the shoulder and quickly froze. The results presented in the table show that the free-stream static temperature at which the run-back freezing occurred experimentally is in good agreement with the analytical values.

The potential hazard to aircraft and missile operation in the transonic region may be seen by applying the results previously given for the critical points at the shoulder of a diamond airfoil to operation under atmospheric conditions likely to be encountered: If a particular relation of pressure and temperature with altitude in the atmosphere is assumed, it is possible to calculate the flight Mach number necessary for icing protection for a given airfoil thickness as a function of altitude. The Mach number necessary for protection for the critical point ahead of the shoulder for a 6-percent-thick diamond airfoil is shown in figure 4 for NACA standard atmosphere (reference 11). For these conditions the region of icing hazard exists from approximately 7500 to 27,300 feet. If a more severe temperature relation with altitude is used such as might be encountered during winter, that is, a 32° F sea-level surface temperature and a lapse rate of 3° F per thousand feet, then the curves shown result for the critical points at the shoulder. For these conditions the region of hazard exists from sea level to 24,000 feet. A M_0 of 1.29 is needed at the peak altitude in order to provide protection.

Although the results presented in this report apply only to the symmetrical-diamond airfoil at zero angle of attack, they may be used as an indication of the region of icing hazard and hence serve as a guide for determining where de-icing systems are needed or what flight plan may be used to prevent icing.

SUMMARY OF RESULTS

The results of the analysis of icing limit presented for the diamond airfoil at zero angle of attack in the transonic-supersonic speed range are as follows:

1. The critical point for the whole airfoil in terms of the icing limit was located immediately behind the shoulder. The critical point on the front surface was located immediately ahead of the shoulder. The results indicate that icing may occur at the critical point behind the shoulder for Mach numbers as high as 1.4.

2. At a constant free-stream Mach number and airfoil thickness, the minimum free-stream static temperature corresponding to an ice-free condition increases with increasing altitude,

3. For the point immediately ahead of the shoulder the minimum free-stream temperature corresponding to an ice-free condition remains the same or decreases with increasing thickness ratio at a constant value of Mach number and altitude. For the point immediately downstream of the shoulder the free-stream temperature corresponding to an ice-free condition increases with increasing thickness at a constant Mach number and altitude.

Lewis Flight Propulsion Laboratory
National Advisory Committee for Aeronautics
Cleveland, Ohio, July 24, 1952

REFERENCES

1. Hardy, J. K.: Kinetic Temperature of Wet Surfaces - A Method of Calculating the Amount of Alcohol Required to Prevent Ice, and the Derivation of the Psychrometric Equation. NACA ARR 5H13, 1945.
2. Messinger, B. L.: Equilibrium Temperature of an Unheated Icing Surface as a Function of Airspeed. Preprint No. 342, Presented at I.A.S. Meeting, June 27-28, 1951.
3. Gelder, Thomas F., Lewis, James P., and Koutz, Stanley L.: Icing Protection for a Turbojet Transport Airplane: Heating Requirements, Methods of Protection, and Performance Penalties. NACA TN 2866, 1953.
4. Schaefer, Vincent J.: The Production of Clouds Containing Supercooled Water Droplets or Ice Crystals under Laboratory Conditions. Bull. Am. Meteorological Soc., vol. 29, no. 4, April 1948, pp. 175-182.
5. Dorsch, Robert G., and Hacker, Paul T.: Photomicrographic Investigation of Spontaneous Freezing Temperatures of Supercooled Water Droplets. NACA TN 2142, 1950.
6. Cole, Julian D.: Drag of a Finite Wedge at High Subsonic Speeds. Jour. Math. Phys., vol. 30, no. 2, July 1951, pp. 79-93.
7. Bryson, Arthur Earl, Jr.: An Experimental Investigation of Transonic Flow Past Two-Dimensional Wedge and Circular-Arc Sections Using a Mach-Zehnder Interferometer. NACA TN 2560, 1951.

8. Vincenti, Walter G., and Wagoner, Cleo B.: Transonic Flow Past a Wedge Profile with Detached Bow Wave - General Analytical Method and Final Calculated Results. NACA TN 2339, 1951.
9. Vincenti, Walter G., and Wagoner, Cleo B.: Transonic Flow Past a Wedge Profile with Detached Bow Wave - Details of Analysis. NACA TN 2588, 1951.
10. Moeckel, W. E., and Connors, J. F.: Charts for the Determination of Supersonic Air Flow Against Inclined Planes and Axially Symmetric Cones. NACA TN 1373, 1947.
11. Diehl, Walter S.: Standard Atmosphere - Tables and Data. NACA Rep. 218, 1925.

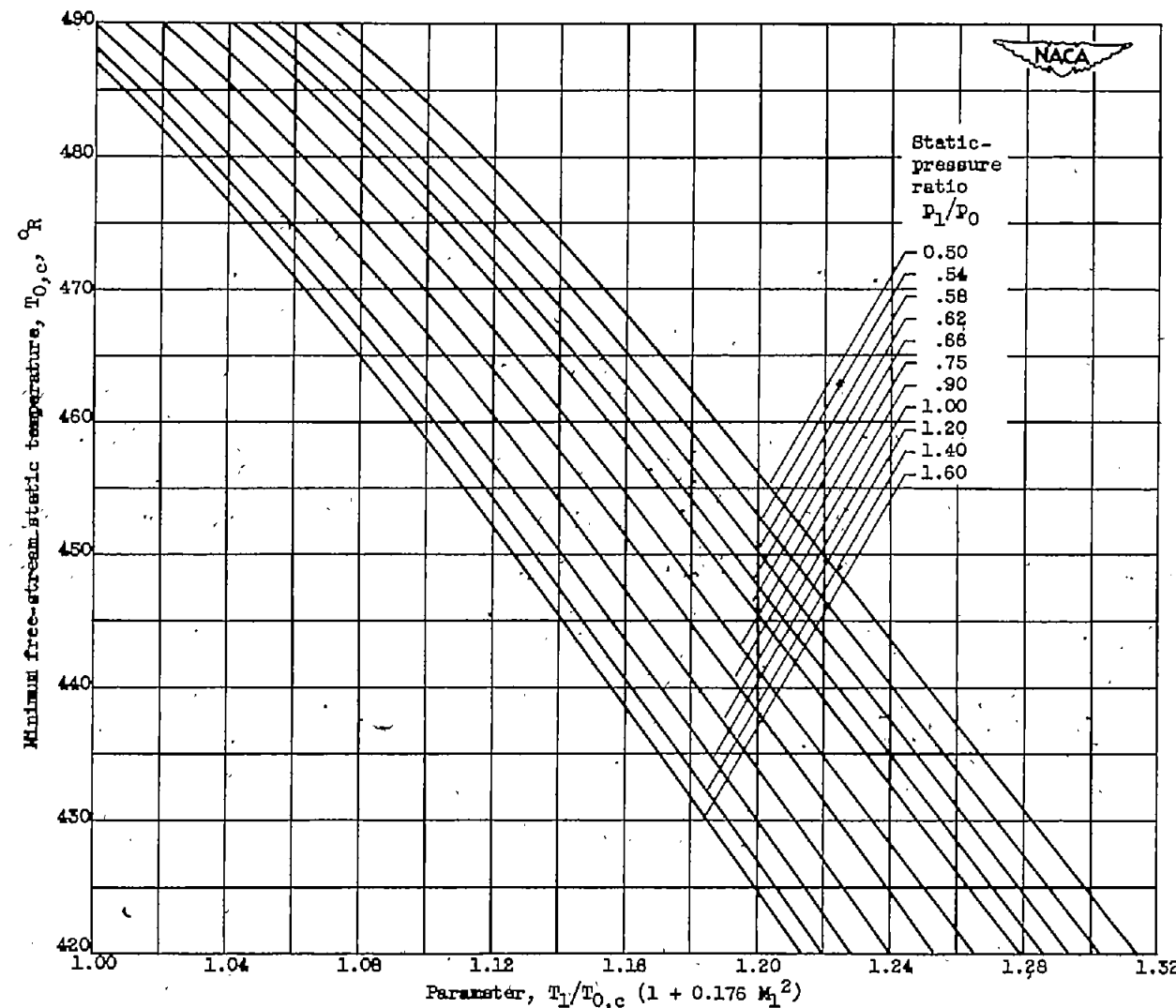


Figure 1. - Variation of free-stream static temperature corresponding to ice-free condition with parameter $T_1/T_{0,c} (1 + 0.176 M_1^2)$ for various static-pressure ratios. Pressure altitude, 15,000 feet.

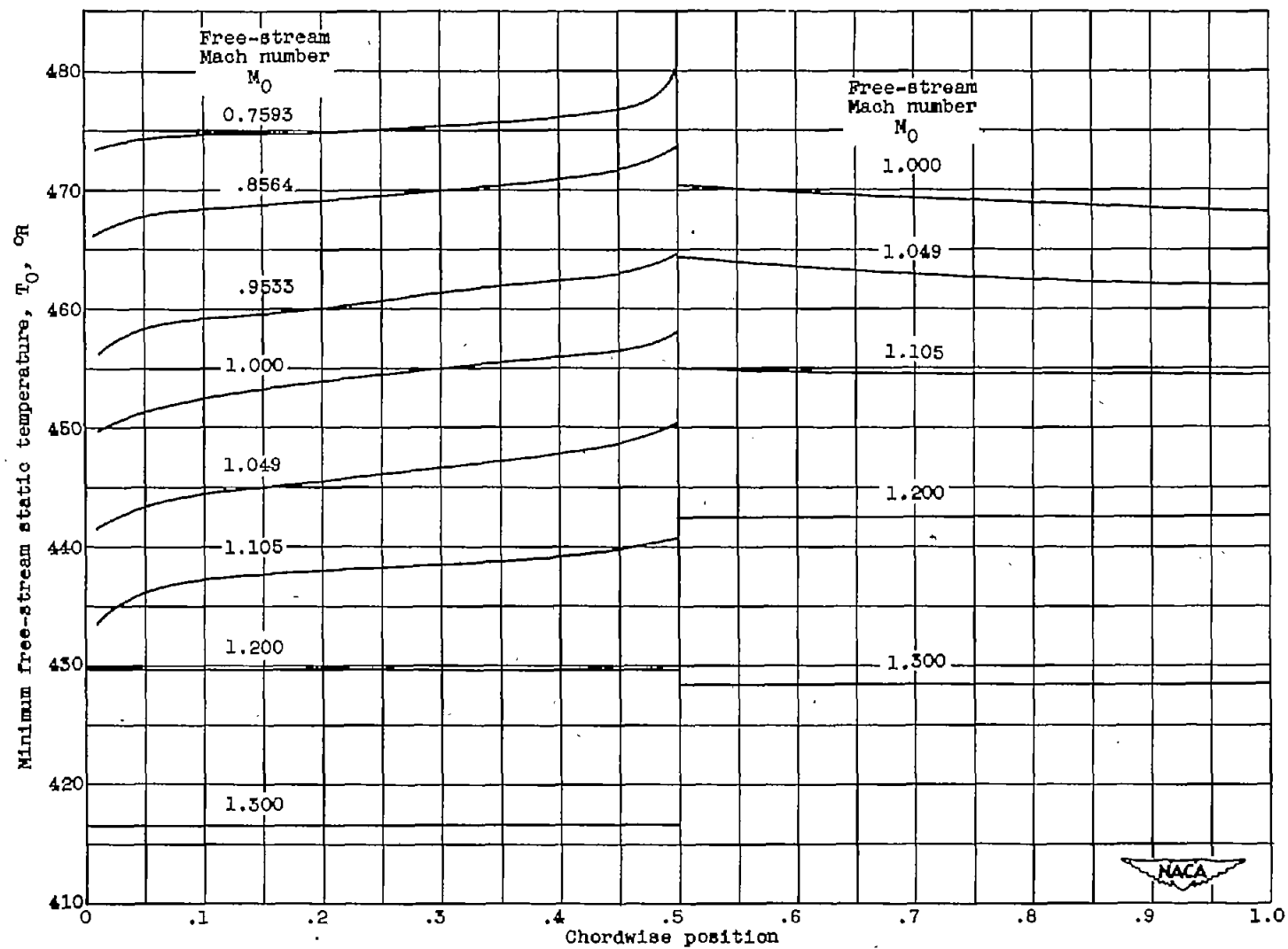
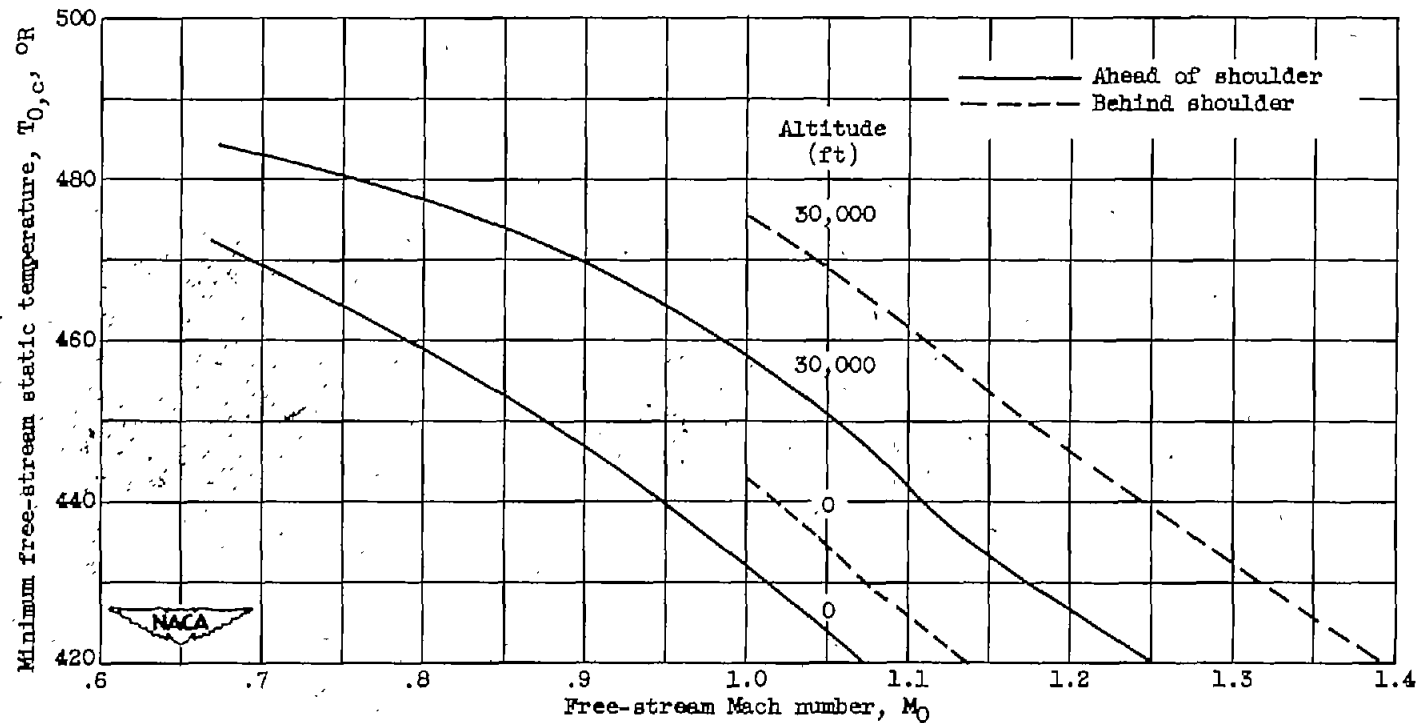
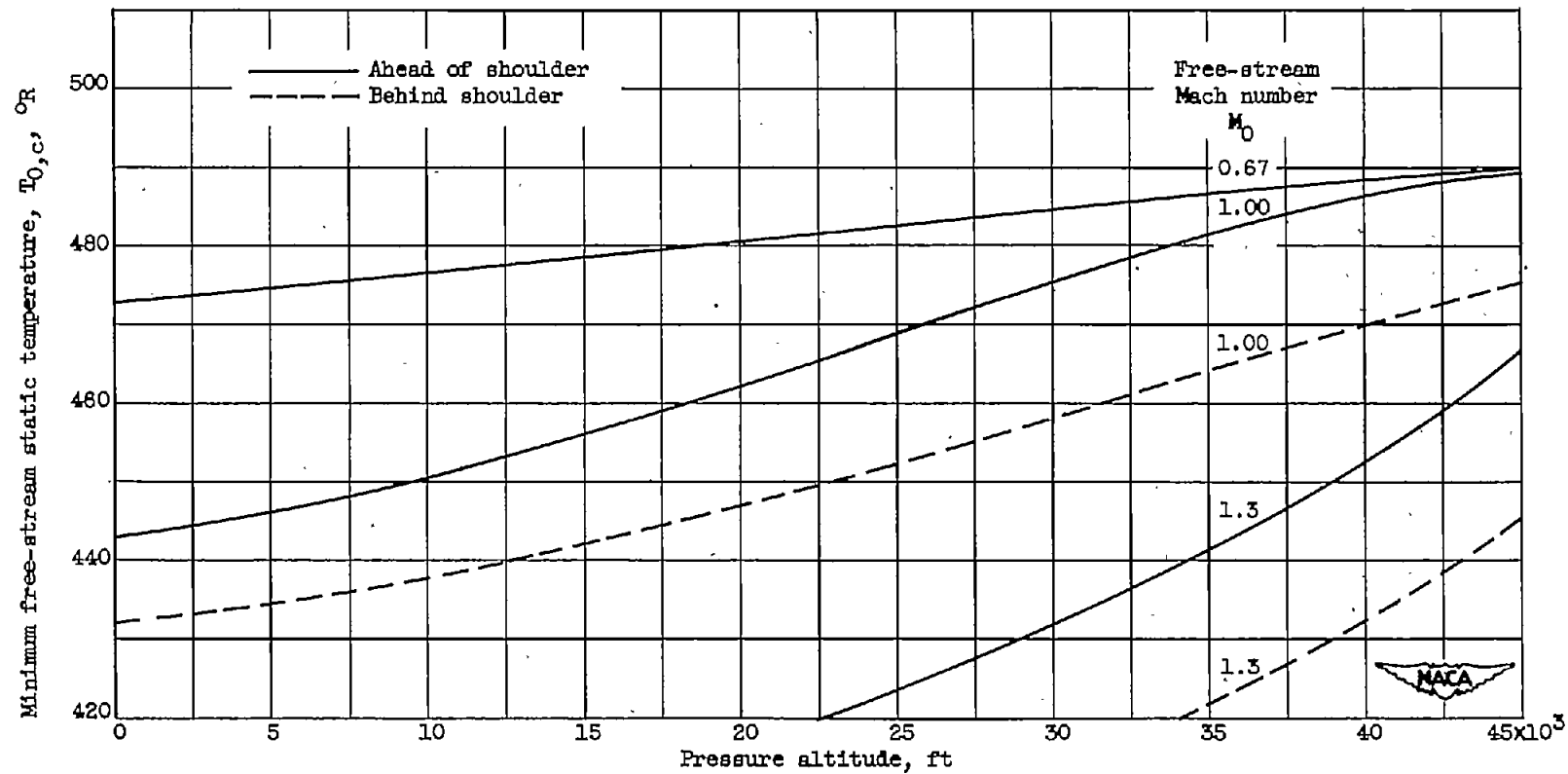


Figure 2. - Chordwise variation of free-stream static temperature corresponding to ice-free condition for several Mach numbers. Airfoil thickness, 4 percent; pressure altitude, 30,000 feet.



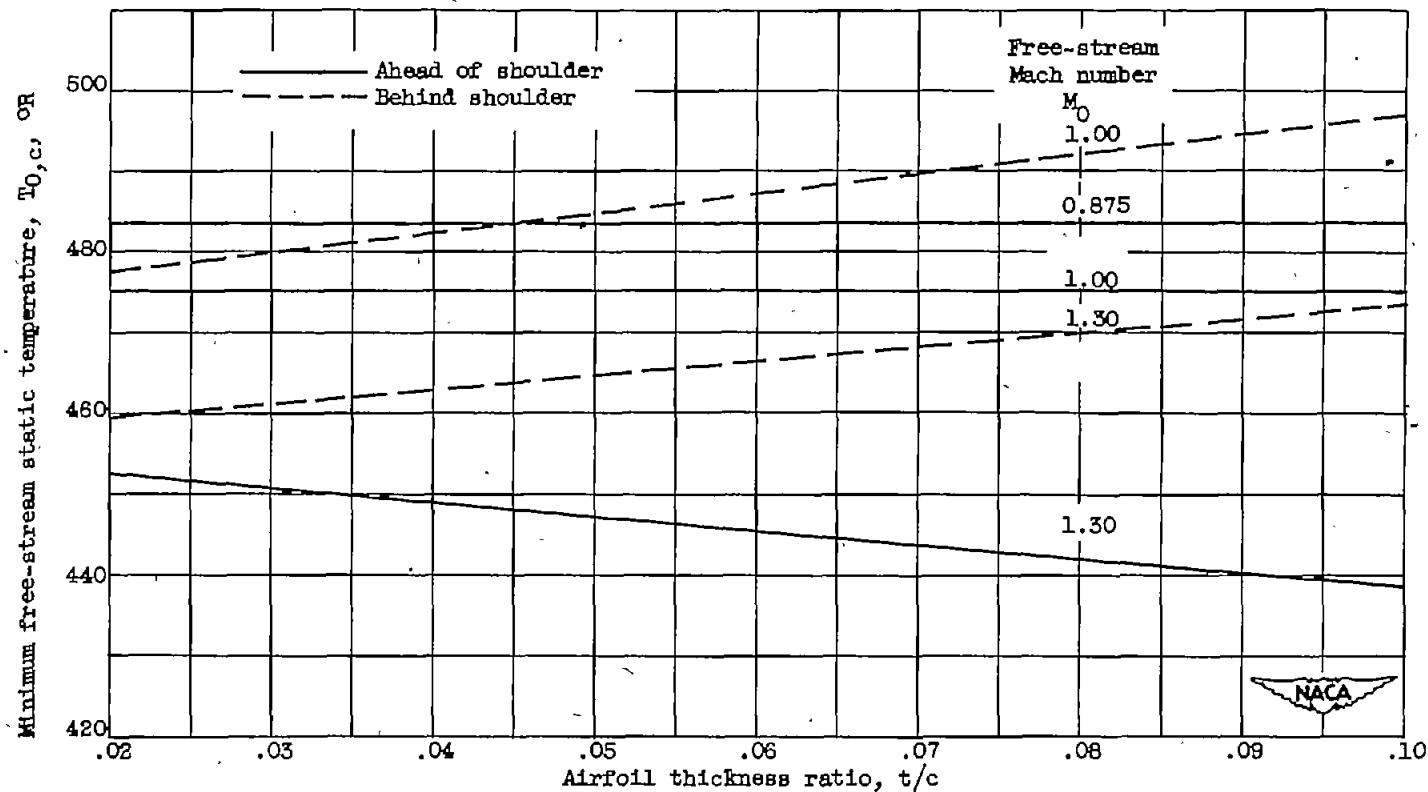
(a) Effect of Mach number. Pressure altitudes, sea level and 30,000; airfoil thickness, 6 percent.

Figure 3. - Variation of minimum free-stream static temperature corresponding to ice-free condition for two critical points on airfoil.



(b) Effect of pressure altitude for several Mach numbers. Airfoil thickness, 6 percent.

Figure 3. - Continued. Variation of minimum free-stream static temperature corresponding to ice-free condition for two critical points on airfoil.



(c) Effect of airfoil thickness for several Mach numbers. Pressure altitude, 45,000 feet.

Figure 3. - Concluded. Variation of minimum free-stream static temperature corresponding to ice-free condition for two critical points on airfoil.

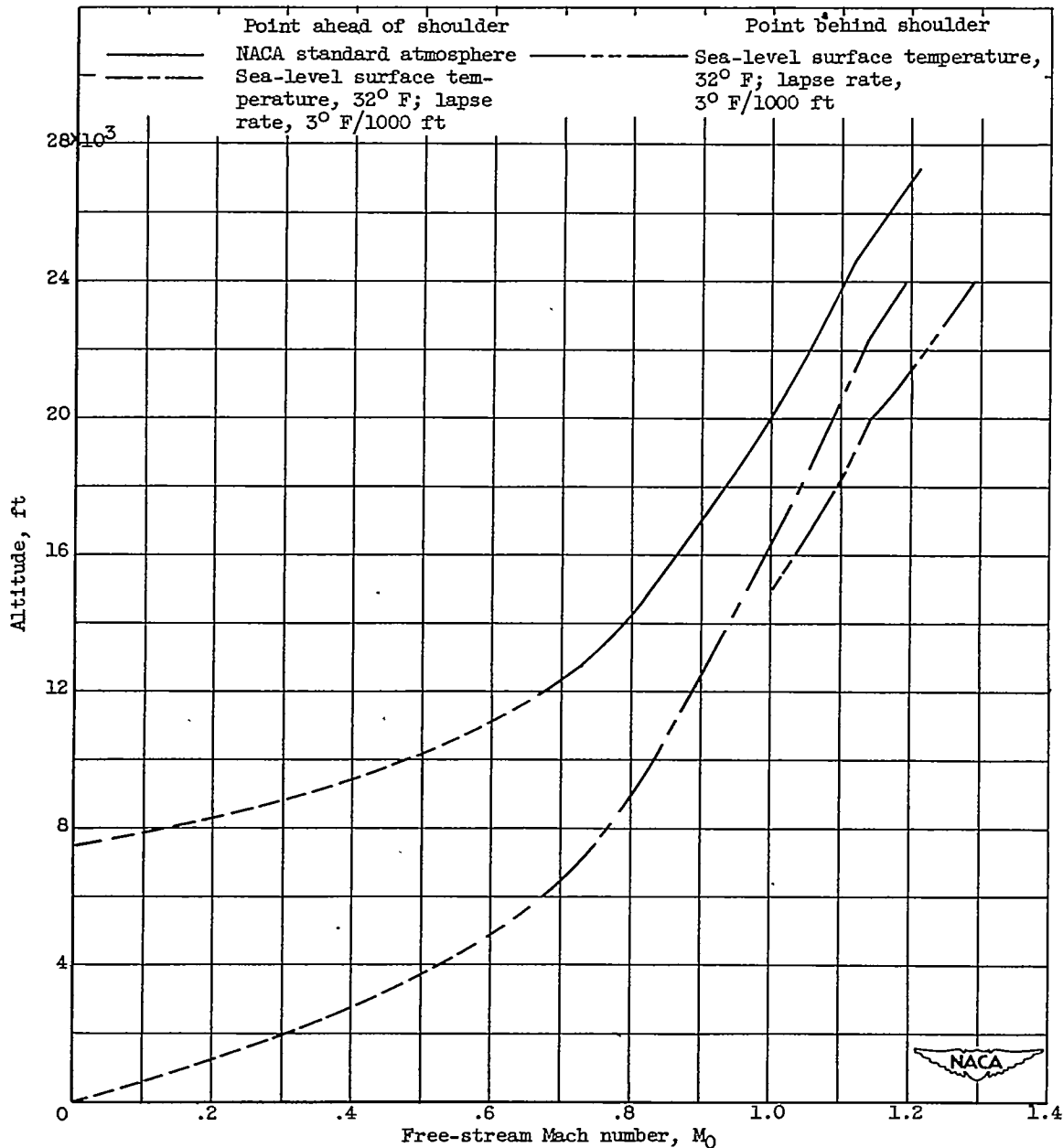


Figure 4. - Variation of flight Mach number required for icing protection as function of altitude for several assumed atmospheric temperature-pressure relations. Airfoil thickness, 6 percent.